

Parameterisation of Cherenkov light production in high-energy showers

F. Nerling^a, J. Blümer^{a,b}, R. Engel^a and M. Risse^a

(a) Forschungszentrum Karlsruhe, Institut für Kernphysik, 76021 Karlsruhe, Germany

(b) Universität Karlsruhe, Institut für Experimentelle Kernphysik, 76021 Karlsruhe, Germany

Presenter: F. Nerling (frank.nerling@ik.fzk.de), ger-nerling-F-abs1-he14-oral

A new analytical description of Cherenkov light production in high energy showers is presented. It describes both the total amount and the angular distribution of the emitted Cherenkov photons as a function of the shower age. A universal parameterisation of electron energy distribution is used for calculating the total number of Cherenkov photons. Based on universality features of the angular distribution of electrons, a parameterisation of produced Cherenkov photons for a given angle to the shower axis is introduced. Thus, a complete analytical description is derived which allows the calculation of direct and scattered Cherenkov contributions to light profiles measured by experiments using the fluorescence technique. The results are compared to CORSIKA simulations and to other parameterisations.

1. Introduction

For correct shower profile reconstruction from light signals measured using the air fluorescence technique, a precise knowledge of the Cherenkov light contribution to the fluorescence detector signal is mandatory. In contrast to the isotropically radiated fluorescence light, the Cherenkov photons are emitted mostly in the forward direction. Therefore, the amount of Cherenkov light in the measured signal depends on the shower geometry with respect to the detector. It leads to systematic uncertainties in the determination of primary properties like energy and position of shower maximum unless accounted for properly. The analytical calculation of the amount of Cherenkov light received by fluorescence detectors needs the total number of Cherenkov photons produced and their angular distribution with respect to the shower axis. The so-called *scattered Cherenkov light* contribution, i.e. those photons which originally would not have reached the detector but are scattered into the field of view, depends mainly on the former and is nearly independent of the shower geometry. The amount of Cherenkov photons directly hitting the detector, the so-called *direct Cherenkov light*, depends on both the total amount of produced Cherenkov photons and their angular distribution with respect to the shower axis.

The total number of Cherenkov photons dN_γ produced per interval of slant depth dX and angle $d\theta$ with respect to the shower axis can be calculated in good approximation by [1, 2]

$$\frac{dN_\gamma}{dX d\theta}(X, \theta, h) = A_\gamma(X, \theta, h) \cdot N(X) \int_{\ln E_{\text{thr}}} y_\gamma(h, E) f_e(X, E) d \ln E. \quad (1)$$

Here, $N(X)$ is the charged particle number as function of depth X , E_{thr} the local Cherenkov energy threshold, which depends on the refractive index $n = n(h)$ of air, and $f_e(X, E)$ is the differential electron energy spectrum at depth X normalised to unity above the energy threshold E_{cut} adopted in the simulation (1 MeV in the examples shown here), cf. [1, 2]. $A_\gamma(\theta, X, h)$ is the angular distribution of Cherenkov photons per angular bin with respect to the shower axis, normalised to one photon and averaged over azimuth

$$A_\gamma(\theta, X, h) \cdot \frac{dN_\gamma}{dX} = \frac{dN_\gamma}{d\theta dX}(\theta, X, h), \text{ with } \int_0^\pi A_\gamma d\theta = 1. \quad (2)$$

For a given shower geometry, $h = h(X)$ follows from the atmospheric model (US-StdA used in the following).

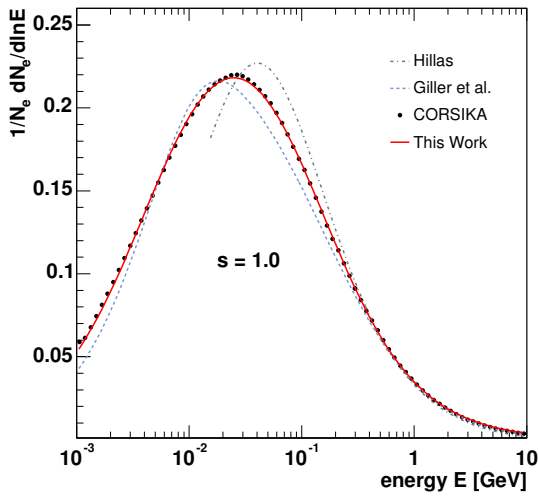


Figure 1. Mean electron energy spectrum CORSIKA, different parameterisations (see text) for $s = 1.0$.

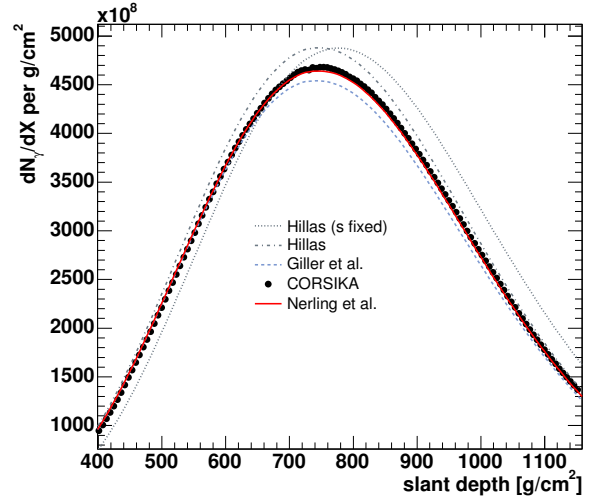


Figure 2. Longitudinal Cherenkov photon profile obtained by CORSIKA, different parameterisations (see text).

2. Total number of Cherenkov photons produced

Applying a parameterisation of the electron energy spectrum, the total number of Cherenkov photons produced per slant depth dX can be calculated analytically based on ansatz (1) when the shower size profile is provided by EAS simulations or by fluorescence observations. A parameterisation of the electron energy spectrum depending only on the shower age $s = 3X/(X + 2X_{\max})$ was first provided by Hillas [3]. Two new approaches have recently proposed [4, 1] based on CORSIKA [5] simulations applying QGSJET01 [6] as interaction model. For high-energy showers $> 10^{17}$ eV, the electron spectrum has shown to be universal, i.e. it does not depend significantly on the primary energy or particle type [4, 1, 2] and is also largely independent of the shower zenith angle [2]. In Fig. 1 different parameterisations of the electron energy spectrum are compared to the Monte Carlo result for $s = 1$. The comparison of the full Monte Carlo Cherenkov profile calculation with the model calculation applying the different parameterisations for ansatz (1) is shown in Fig. 2. The parameterisation given by Nerling et al. also accounts for different E_{cut} , which is important to be consistent with $N(X, E > E_{\text{cut}})$. The calculation labelled “Hillas (s fixed)” employs the parameterisation given in [3] for $s = 1$ only, as often used (see e.g. [7, 8]).

3. Angular distribution of electrons and Cherenkov photons

Electrons in a shower undergo multiple Coulomb scattering, which broadens their angular distribution with respect to the shower axis: The higher the mean electron energy, the smaller is the mean electron angle to the shower axis. In Fig. 3 the energy dependent angular distribution of electrons is shown exemplarily for an individual proton shower of 10^{19} eV for three different shower ages. It can be seen that the distribution is strongly depending on the particle energy, and is to a large extent independent of the shower age within the statistical fluctuations. As the electron energy spectra are universal in high-energy showers and the electron scattering angle is mostly determined by the particle energy, the electron angular distribution is also approximately independent of shower energy and primary particle type [2]. This is illustrated in Fig. 4 where the electron angular distributions of many individual proton and iron showers of different energies ($10^{18}, 10^{19}$ eV) are shown at

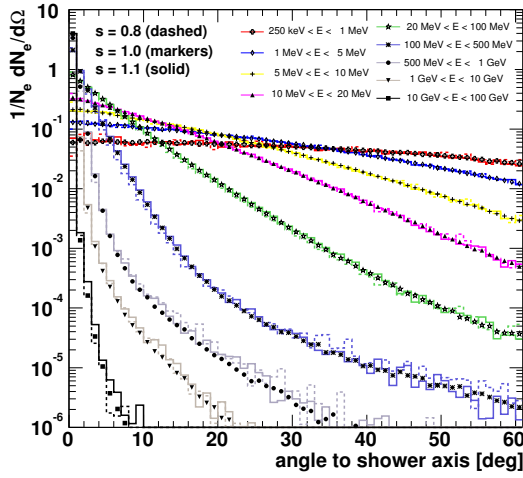


Figure 3. Normalised electron angular distribution with respect to the shower axis, shown for an individual proton shower of 10^{19} eV for three different shower ages and various different ranges of electron energies.

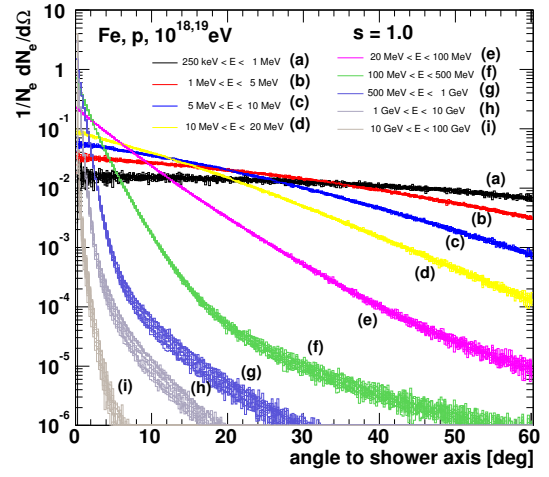


Figure 4. Universality of electron angular distributions, shown for numerous individual proton and iron showers of 10^{18} and 10^{19} eV and various different ranges of electron energies.

shower maximum, cf. also [9]. The distributions of individual showers do not differ much, larger (statistical) fluctuations occur merely at large angles. The distribution of electrons in the GeV-region show a larger spread, which is in agreement with the energy spectra of GeV-electrons showing larger fluctuations as well [2].

The Cherenkov photons are emitted under the Cherenkov emission angle, which slightly changes with altitude and amounts about 1° in air. This angle is negligible compared to the broad distribution of electrons. Consequently, the Cherenkov photon angular distribution is determined mainly by the electron energy spectrum and two dependencies occur. The photon angular distribution depends on height h due to the dependence of $E_{\text{thr}}(h)$, and on the shower age s because of the dependence of $f_e(E, s)$. It is common to describe the height dependence by an exponential function, where the scaling angle θ_0 is a function of E_{thr} , see e.g. [7]. Traditionally this approximation is applied for calculating the Cherenkov contamination of fluorescence light signals from high-energy showers, see e.g. [7, 8]. Generalising this ansatz in order to take into account both the dependence on h as well as on s we write $A_\gamma(\theta, h, s) = A_\gamma(s) \cdot A_\gamma(\theta, h)$, where $A_\gamma(s)$ is a polynomial of second order in shower age and the exponential term depends on altitude only. To enlarge the range of validity up to 60° and improve the data description around 30° this factorised ansatz is extended to [2]

$$A_\gamma(\theta, h, s) = a_s(s) \frac{1}{\theta_c(h)} e^{-\theta/\theta_c(h)} + b_s(s) \frac{1}{\theta_{cc}(h)} e^{-\theta/\theta_{cc}(h)}. \quad (3)$$

In this expression, the age dependence is included by the polynomials $a_s(s)$ and $b_s(s)$, and the height dependence is taken into account by $\theta_c(h) = \alpha \cdot E_{\text{thr}}^{-\beta}$ and $\theta_{cc}(h) = \gamma \cdot \theta_c(h)$ with $\gamma = \alpha' + \beta' \cdot s$, where E_{thr} is given in MeV. As shown in Fig. 5 and Fig. 6 respectively, the CORSIKA results are described properly using the parameters given in [2].

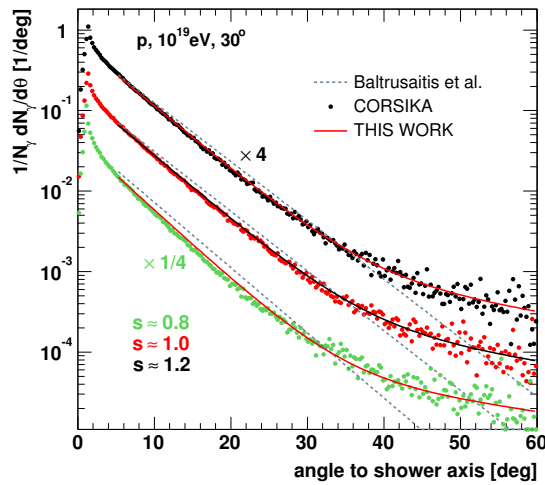


Figure 5. Angular distribution of Cherenkov photons with respect to the shower axis. Shown are the simulated distributions for an individual proton shower for different shower ages, [7] and the new parameterisation Eq. (3) [2].

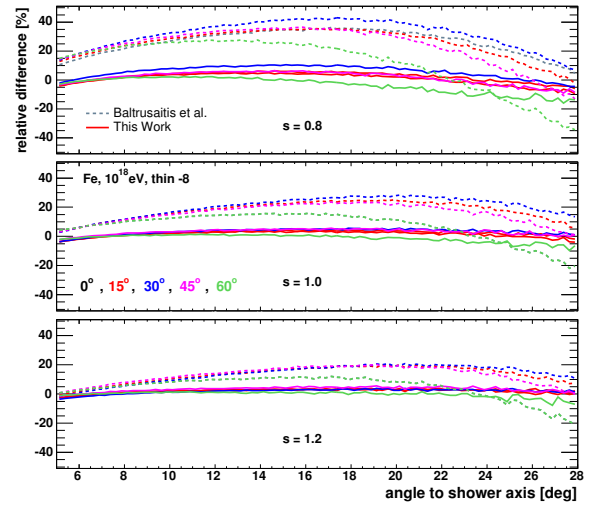


Figure 6. Quality of description: Relative differences of different approaches ([7] and Eq. (3) [2]) to CORSIKA results, shown for 5 individual iron showers and different zenith angles.

4. Conclusions

Based on universality features of high-energy showers, an analytical description of the Cherenkov light production in EAS has been introduced providing both, the total number of produced Cherenkov photons as well as their angular distribution with respect to the shower axis. It offers the calculation of the direct and scattered Cherenkov contributions to measured fluorescence light profiles, see [10]. The achieved accuracy in reproducing the CORSIKA predictions in terms of the number of Cherenkov photons produced per slant depth and angle with respect to the shower axis is (within shower-to-shower fluctuations) better than a few percent ($< 10\%$ for $s=0.8$, $< 5\%$ for $s=1.0$, $< 3\%$ for $s=1.2$). The differences compared to the traditionally used approach result in significant and systematic differences in reconstructed energy and position of shower maximum, if the new model is applied for shower profile reconstruction as has been shown for Auger hybrid data [10].

References

- [1] F. Nerling et al., Proc. 28th Int. Cos. Ray Conf., Tsukuba (Japan), 2 (2003) 611.
- [2] F. Nerling et al., astro-ph/0506729 (2005).
- [3] A. M. Hillas, J. Phys. G: Nucl. Part. Phys. 8 (1982) 1461.
- [4] M. Giller et al., J. Phys. G: Nucl. Part. Phys. 30 (2004) 97; Proc. 28th Int. Cos. Ray Conf., Tsukuba (Japan), 2 (2003) 619. Note: Parameters used here are different from that published, a new set of parameters [Giller et al. 2005, private communication] is used.
- [5] D. Heck et al., Report FZKA 6019, Forschungszentrum Karlsruhe (1998).
- [6] N. N. Kalmykov, S. S. Ostapchenko, A. I. Pavlov, Nucl. Phys. B (Proc. Suppl.), 52B (1997) 17.
- [7] R. M. Baltrusaitis et al., Nucl. Instr. Meth. A 240 (1985) 410.
- [8] T. Abu-Zayyad et al., HiRes Collaboration, Astropart. Phys., 16 (2001) 1.
- [9] M. Giller et al., Int. J. Mod. Phys. A: Proc. 19th European Cos. Ray Symp., Florence (Italy) (2004).
- [10] F. Nerling et al., Pierre Auger Collaboration, these proceedings, ger-nerling-F-abs2-he14-poster (2005).